

E. ZEEK<sup>✉</sup>  
A.P. SHREENATH  
P. O'SHEA  
M. KIMMEL  
R. TREBINO

# Simultaneous automatic calibration and direction-of-time removal in frequency-resolved optical gating

School of Physics, Georgia Institute of Technology, Atlanta, GA 30332, USA

Received: 20 September 2001/  
Revised version: 13 November 2001  
Published online: 16 July 2002 • © Springer-Verlag 2002

**ABSTRACT** We show that replacing the usual beam splitter with an etalon yields a simple method for automatically calibrating both the delay and the frequency axes of any frequency-resolved-optical-gating (FROG) device. It also simultaneously removes the direction-of-time ambiguity in second-harmonic-generation FROG.

PACS 42.79.Ho

## 1 Introduction

The complete temporal measurement of ultra-short laser pulses, an unsolved problem only a decade ago, has become very nearly routine. Techniques, such as frequency-resolved optical gating (FROG) [1–3] (see Fig. 1), have made such measurements not only possible, but also straightforward. FROG is quite simple to implement but, as with any technique, one would like to eliminate the most arduous features, which also represent potential sources of error.

One such task is the calibration of the relevant axes, which is arduous in almost any technique and can always yield errors. FROG measurements are functions of both delay and frequency, whose increments of delay per pixel and wavelength per pixel, respectively, must be determined. Miscalibration of one or both axes can yield a high retrieval error and/or incorrect results. Another task in the second-harmonic-generation (SHG) version of FROG is the removal of the ambiguity in the direction of time. While other versions of FROG uniquely determine the pulse, the pulse and its mirror image yield the same trace in SHG FROG, so one must perform additional measurements to determine which pulse field is correct [3]. Although FROG contains checks and balances on all measurements [1], a method for automatic calibration and the removal of this ambiguity would be welcome.

In this paper, we describe a simple and elegant method for simultaneously solving both of these problems, which we call procedure for objectively learning the calibration and direction of time (POLKADOT) FROG. POLKADOT FROG can

be implemented in several different ways. We discuss various geometries that solve these problems, including one that can be turned on and off with a single knob.

Consider the calibration problem first. Our solution is inspired by the FROG trace of a double pulse, as shown in Fig. 2. This trace contains three islands of intensity, each separated by the pulse separation,  $\tau_{\text{sep}}$ , just as in an autocorrelation of a double pulse, shown as the delay marginal. However, in FROG, the islands are also frequency-resolved. Moreover, in FROG the central island has fringes in frequency with a separation of  $1/\tau_{\text{sep}}$ , as illustrated in the frequency marginal. Thus, the pulse separation determines the spacing of the main structure of the double-pulse FROG trace in both delay and frequency. Thus, propagating a double pulse with known pulse spacing into a FROG device automatically yields the increments of both delay and frequency per pixel and hence calibrates the FROG device. This method works even when the pulse has structure to begin with, provided that the separation of the double pulse is greater than the width of the individual pulses.

Accordingly, our solution involves generating a double pulse and identifying these islands and their separation in the resulting trace. This can easily be done by simply placing an etalon of known optical thickness in the beam before the FROG device. Of course, an etalon produces an infinite train of pulses, but a sufficiently low etalon reflectivity yields essentially one additional pulse – all that is needed.

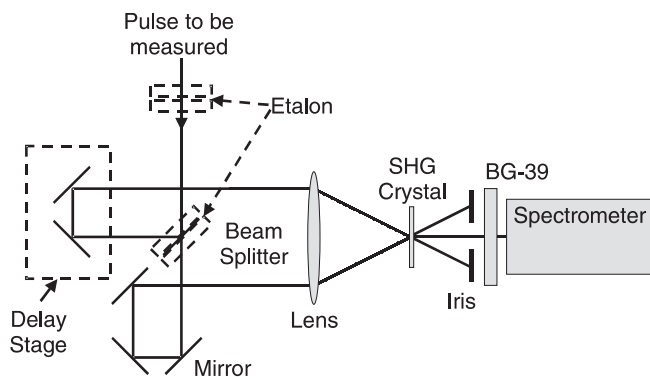


**FIGURE 1** FROG Device Schematic. A schematic layout of an SHG FROG device, showing two possible positions for the etalon in the POLKADOT FROG arrangement, both of which automatically calibrate the device and remove the ambiguity in the direction of time

✉ Fax: +1-404/894-9958, E-mail: erik.zeek@physics.gatech.edu

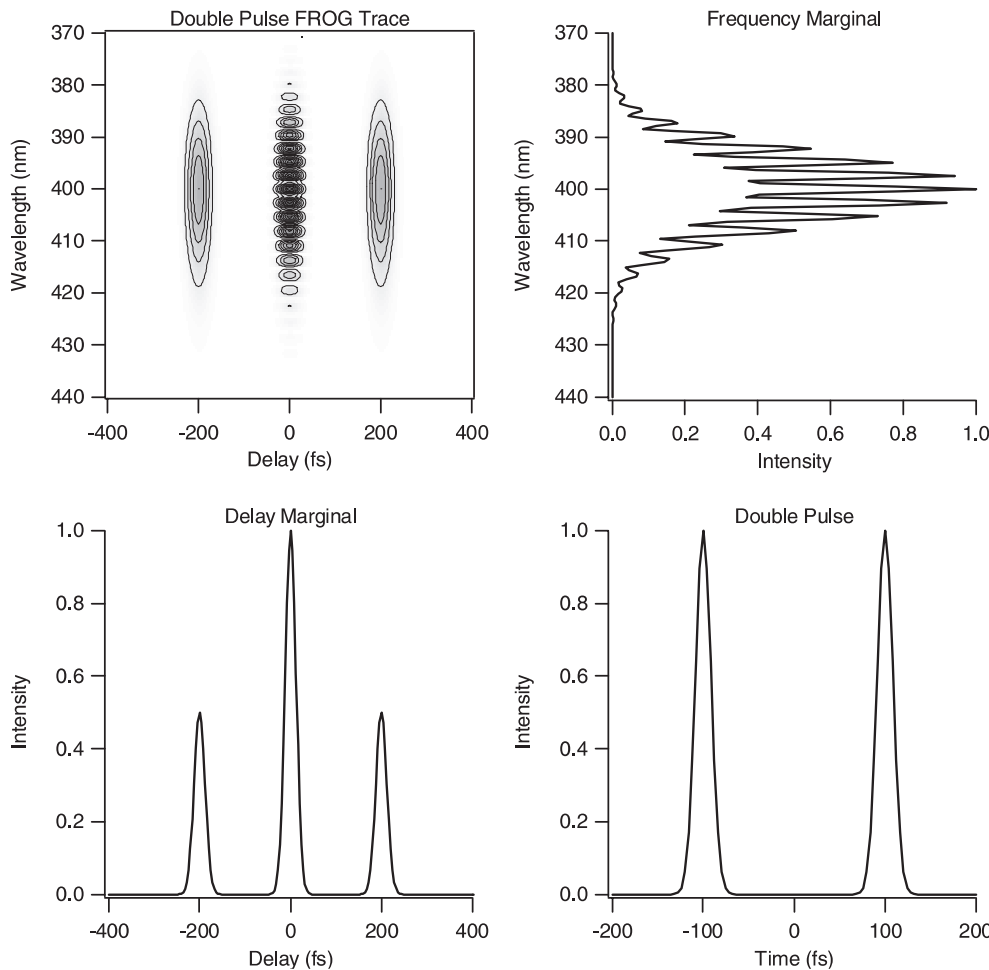


**FIGURE 2** Double Pulse FROG Trace. This figure shows the SHG FROG trace for two 20-fs pulses separated by 200 fs (The pulse train is shown in the lower right-hand corner.) The trace in the upper left shows the square root of the FROG intensity,  $I_{\text{FROG}}$ . Also shown are the two marginals (integrals of the trace with respect to delay or frequency) that exhibit characteristic modulations

While the above solution is quite simple, a more elegant solution is to replace the usual beam splitter in the FROG device with an etalon (see Fig. 1). The etalon's front and back reflectivities must be carefully chosen in order to yield identically shaped pulses in both arms of the FROG device, so that the usual pulse-retrieval algorithm will operate effectively. This is because the algorithm assumes that the shapes of the two pulses are identical (the pulse energies may, however, be different). Specifically, the ratio of the first and second pulse energies in each pulse train should be the same. It is easy to show (see Appendix A) that this ratio will be the same for both arms as long as the front surface has a 50% reflectivity. Interestingly, the back-surface reflectivity cancels out of this result and hence is arbitrary, so we have chosen a value of about 10% for our experiments in order to minimize the additional pulses in the train and to minimize the wasted energy in such pulses. For a back-surface reflectivity of 10%, the second pulse in each arm has 5% of the energy of the first pulse. Note that, despite the weakness of the second pulse, the frequency fringes remain strong: their relative amplitude is given by the geometric mean of the first and second pulse energies, which is 45% in the above example. Finally, for these values of the reflectivities, the third pulse has an energy of 0.25% of the first pulse and hence is negligible. (It does introduce slight fringes in the outer islands, which can in fact be used to check the calibration.)

This replacement also solves the direction-of-time ambiguity in SHG FROG. The second pulse is necessarily weaker than the first, so it is impossible to confuse the retrieved pulse with its weaker trailing pulse from its mirror image, whose weaker pulse leads the stronger one. An etalon has been used to determine the direction of time previously [4], but not with the etalon as a beam splitter nor in conjunction with an auto-calibration scheme.

POLKADOT FROG requires no change in the FROG pulse-retrieval algorithm. It only requires a somewhat larger scan range (to see the extra islands) and a slightly better spectral resolution (to resolve the spectral fringes). This increase in range/resolution is not significant, as it is not necessary to accurately acquire the details in the wings of the additional islands or in the spectral fringes, but instead only to find their separations.

## 2 Autocalibration

For the purpose of automatic calibration, we have written a simple code to find the peaks in the trace. This code does not require the use of the entire FROG trace. Instead, it simply requires computing the frequency and delay marginals (integrals of the trace with respect to delay and frequency, respectively). It then uses a simple peak-finding routine to obtain an initial guess of the peak locations and then curve-fits

the marginals to a sum of Gaussians. The functional form of the equations is

$$FIT = a + b\tau + c_{\text{back}} e^{-((\tau-x_{\text{back}})/w_{\text{back}})^2} + \sum_{j=0}^n c_j e^{-((\tau-x_j)/w_j)^2} \quad (1)$$

where  $a + b\tau$  accounts for a flat background with perhaps some slope,  $c_j$  is the amplitude of a Gaussian peak,  $x_j$  is the center of the peak, and  $w_j$  is the width of the peak. Also included is a background Gaussian peak, with the  $c_{\text{back}}$ ,  $x_{\text{back}}$ , and  $w_{\text{back}}$  parameters. This Gaussian takes into account possible pulse-shape variations and insufficient resolution. This is especially important for the frequency marginal, which has small peaks on top of a large peak. The important information in this equation is contained in the  $x_j$  parameters. These parameters define the centers of the peaks, and contain the information needed to calibrate the FROG trace. Of course, only one such peak is necessary in each direction, but two or even four or more yield statistical data, which can be fitted for even better results.

Given the peak centers, it is a simple matter to calculate the calibrations of the FROG trace. The delay spacing,  $d\tau$ , is simply

$$d\tau = \frac{\tau_{\text{sep}}}{S_\tau}, \quad (2)$$

where  $\tau_{\text{sep}}$  is the peak-to-peak separation in time and  $S_\tau$  is the peak-to-peak separation in pixels. The wavelength spacing,  $d\lambda$ , is slightly more complicated:

$$d\lambda = \frac{\lambda_0^2}{\tau_{\text{sep}} S_\lambda c}, \quad (3)$$

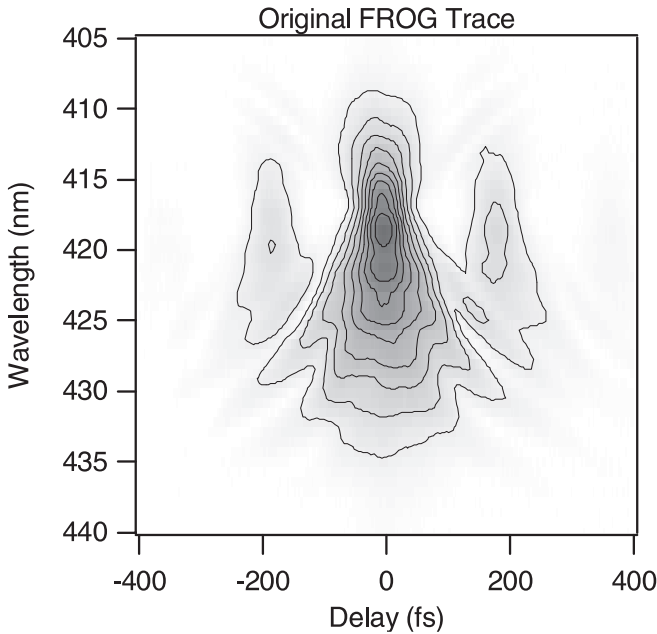


**FIGURE 3** POLKADOT FROG Trace. This is the  $\sqrt{I_{\text{FROG}}}$  of an SHG FROG trace using a 50% / 10% etalon as a beam splitter as described in the text

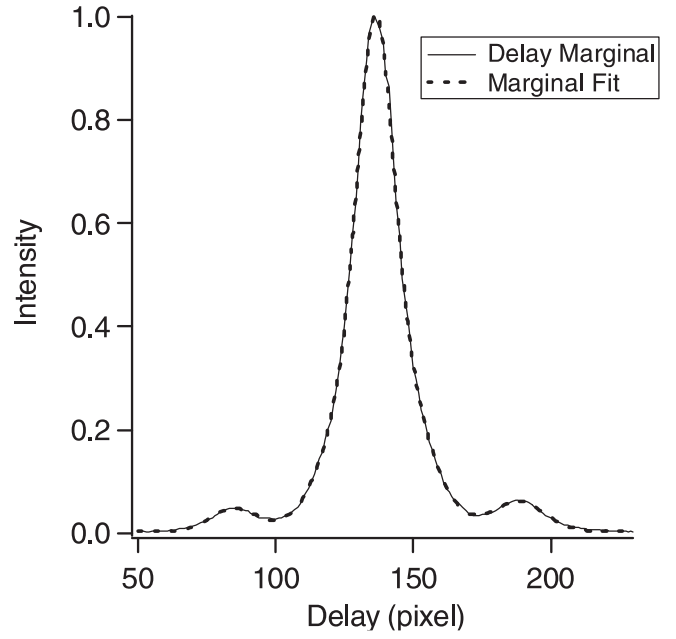


**FIGURE 4** Delay Marginal (equal to the pulse intensity autocorrelation). The delay marginal has peaks separated by the pulse separation. The fit of Function (1) to the marginal is also shown

where  $\lambda_0$  is the center wavelength of the delay marginal,  $S_\lambda$  is the peak separation, and  $c$  is the speed of light. The  $S_\lambda$  used in these experiments is the average separation. For very broadband pulses, this is not an exact solution; the separation is constant in frequency, not wavelength. When the bandwidth is small, this effect is not significant. The center wavelength,  $\lambda_0$ , must be determined through an independent method, although halving the fundamental's center wavelength is probably sufficient for most purposes.

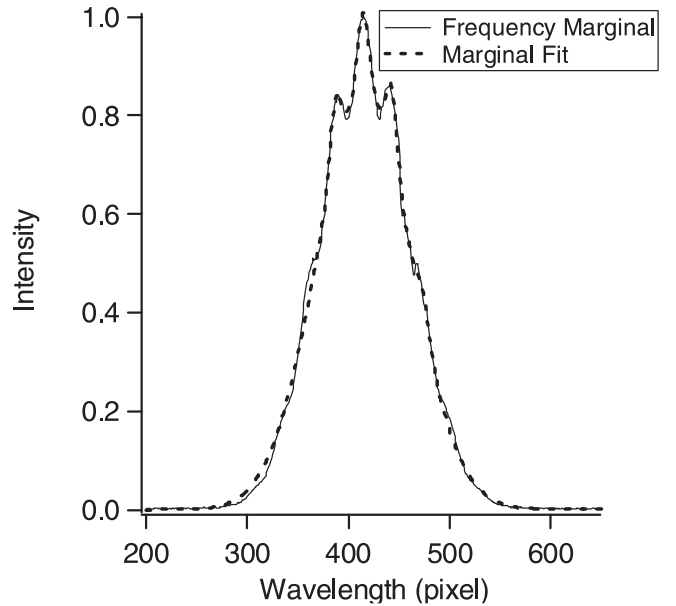


**FIGURE 5** Frequency Marginal (equal to the autoconvolution of the spectrum). The frequency marginal has peaks separated by the reciprocal of the pulse separation. The fit of Function (1) to the marginal is also shown

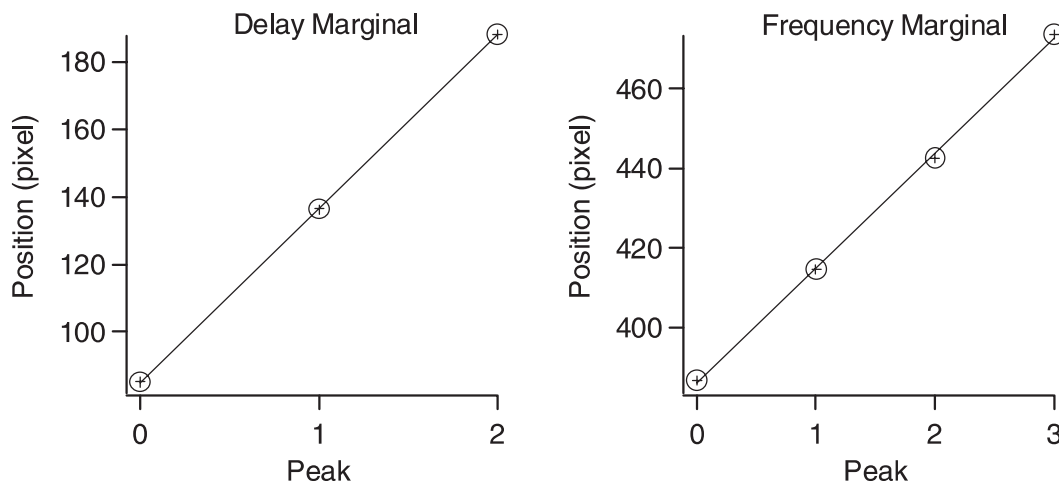


**FIGURE 6** Peak Positions and Calibration Fit Functions. Shown here are the peak positions from the marginals and the straight line fits. The delay marginal fit was  $84. +951x$ , and the frequency marginal fit was  $38 + 628x$ , where  $x$  is the peak number

We tested POLKADOT FROG using a SHG FROG device in which we replaced the usual beam splitter with a  $26.8 \mu\text{m}$  etalon having a 50% first-surface reflectivity and a 10% second-surface reflectivity, as mentioned. The etalon was air-spaced, and the two windows were each 5 mm thick. (It is interesting to note that the etalon beam splitter balances the dispersion of both arms. Since the reflective surface is at the center of the beam splitter, all pulses traverse the same amount of glass, and there is no need for a compensation plate in either arm.) This etalon yielded pulses separated

by 179 fs. The etalon spacing is itself easily calibrated by measuring the spectrum of light transmitted through it and using the same formula as above for the fringe spacing. To measure this we used a commercial spectrophotometer, a Varian Cary 500 Scan, and fitted the peaks using a simple LabVIEW code.

The SHG FROG device in these experiments used a  $100 \mu\text{m}$  thick KDP crystal and a beam angle of  $\sim 5^\circ$ . The delay was stepped using a Newport MFN25PP translation stage and an ESP 300 controller. The spectrometer was an Acton

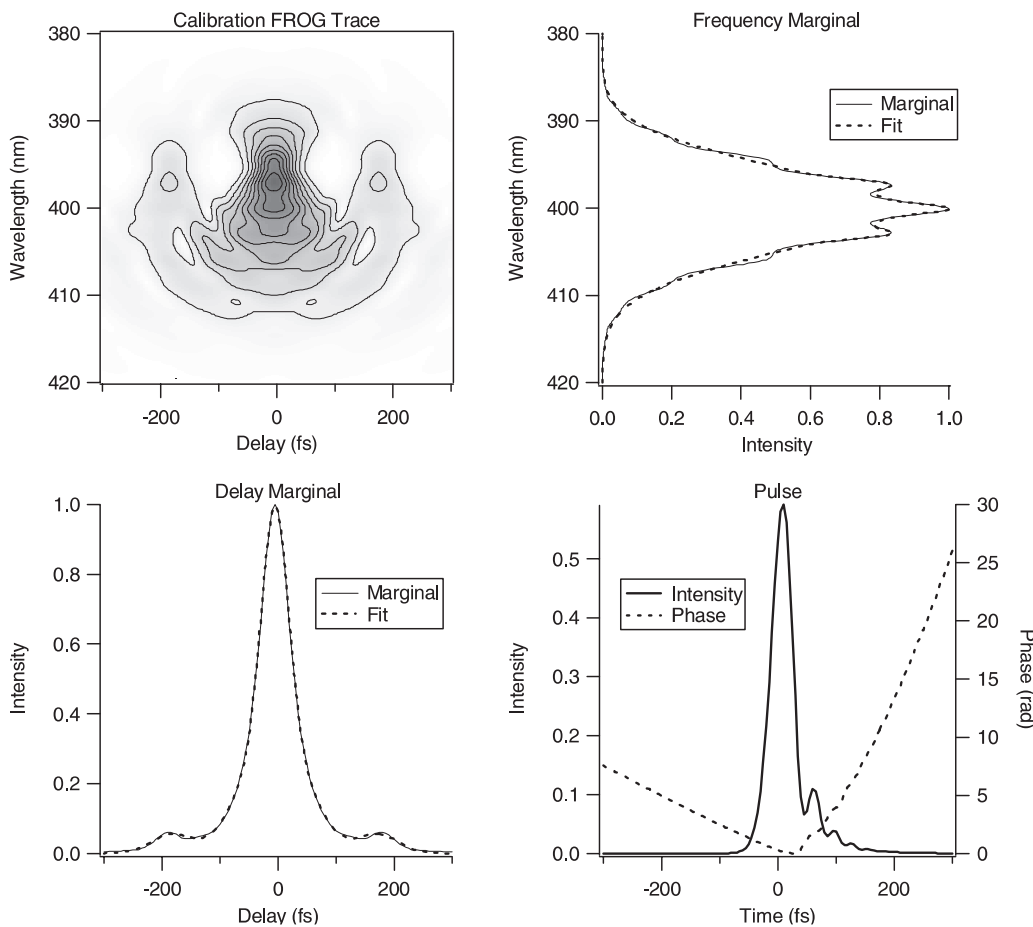


**FIGURE 7** A Complicated Theoretical POLKADOT FROG Trace. The POLKADOT FROG trace in the *upper left* was created from the pulse in the *lower right*, assuming that the pulse had passed through a 50% / 10% etalon that created a pulse separation of 180 fs. Again, the square root of  $I_{\text{FROG}}$  is shown in the *upper left*. The original trace had a time calibration of 5000 fs/pixel and a spectral calibration of 0.1043 nm/pixel. The retrieved calibrations were 5067 fs/pixel and 0.1065 nm/pixel

Research Spectra Pro 150 with a 1200 gr/mm grating. An Oriel Instaspec II pda camera was used to acquire the spectra.

We deliberately used a somewhat distorted pulse, whose FROG trace obtained using POLKADOT FROG is shown in Fig. 3. It clearly shows one pair of additional islands. The marginals for the FROG trace are shown in Fig. 4 (the delay marginal) and Fig. 5 (the frequency marginal). Fitting (1) to each set of marginals, we determined the peak locations, shown in Fig. 6. The fitting was performed by Matlab code developed for this purpose. For both marginals, we were able to obtain more than one set of additional peaks. Using a simple linear fit, we determined the average spacing between the peaks. For the delay marginal, the spacing was  $51.6 \pm 0.2$  pixels and, for the frequency marginal, the spacing was  $28.9 \pm 0.5$  pixels. This yields a temporal calibration of  $3.47 \pm 0.01$  fs/pixel and a frequency calibration of  $0.106 \pm 0.002$  nm/pixel, using 405 nm as the center wavelength. Both axes were also calibrated through more traditional means. The delay calibration was read directly from the encoder on the translation stage. The step size was  $0.518 \mu\text{m}$ , which yields a temporal spacing of 3.46 fs/pixel. The spectrometer was calibrated using a Kr-vapor lamp. By fitting several spectral lines, the spacing was found to be 0.1067 fs/pixel. The etalon calibration values are easily within experimental error of the independently determined values.

We have also simulated the performance of this device on a complex pulse; in particular, a pulse with a Gaussian spectrum and spectral quadratic and cubic phase, shown in Fig. 7. In this case, the pulse has structure that could, in principle, confuse the fitting procedure. However, the FROG trace and the resulting marginals smooth out this structure, leaving only the desired structure. In addition, it must be admitted that pathological cases in which the pulse is in fact a double pulse separated by approximately the etalon round-trip time can confuse this procedure. One is cautioned not to use such pathological pulses in the calibration stage.

Overall, we found this approach to calibration quite satisfying. It is more reliable for the delay calibration than the use of a commercial translation-stage calibration, which is subject to mechanical problems that can be difficult to track down. In one case, a translation stage exhibited different calibrations in different regions of its travel. Thus, a calibration obtained in one region would not have been valid in another. POLKADOT FROG solves this problem and, even better, it involves no moving parts (although there may be moving parts in the FROG device itself), and it continually recalibrates the device for every measurement.

The POLKADOT option can be used in all FROG variations. In addition, it is easy to imagine many other methods for fitting the peaks. For example, one could force the peaks to be equally spaced, thus allowing only one peak-separation parameter. Alternatively, one could incorporate a multiple-pulse formula into the FROG algorithm.

### 3 Removal of the direction-of-time ambiguity

In addition to calibrating the trace, POLKADOT FROG removes the direction-of-time ambiguity from a SHG FROG trace. Figure 8 shows the pulse retrieved from the SHG

FROG trace in Fig. 3. Ordinarily, the retrieved pulse in a SHG FROG measurement would be ambiguous because the pulse obtained by the algorithm and its mirror image yield the same FROG trace (that is, the measured one) and so it is not possible to determine which is correct. However, in this case, we know that the second pulse is much weaker than the first, and we know when it occurs. In the pulse shown in Fig. 8, the secondary pulse must occur at, and is clearly evident at, about 180 fs, and hence is easily identified as the second pulse in the train. Thus, the POLKADOT FROG geometry also eliminates the direction-of-time ambiguity in SHG FROG.

Of course, when one measures a pulse, one wishes to obtain that pulse, not a version of it with a weak second pulse trailing behind it. Fortunately, removal of the second pulse is straightforward. Note that, more precisely, an infinite train of additional pulses follows behind the first pulse, each delayed by  $\tau$  and reduced by a factor of, say,  $\varepsilon$ . Thus POLKADOT FROG yields a measured field,  $E_{\text{meas}}(t)$ , with additional delayed replicas of the pulse field:

$$E_{\text{meas}}(t) = E(t) + \varepsilon E(t - \tau) + \varepsilon^2 E(t - 2\tau) + \dots, \quad (4)$$

where  $E(t)$  is the actual pulse, which we desire. To obtain  $E(t)$ , it is simply necessary to subtract off the measured field reduced in magnitude by  $\varepsilon$  and displaced by  $\tau$ : that is, by subtracting off the quantity  $\varepsilon E_{\text{meas}}(t - \tau)$ . This yields a new quantity:

$$E'_{\text{meas}}(t) = E_{\text{meas}}(t) - \varepsilon E_{\text{meas}}(t - \tau). \quad (5)$$

Substitution of  $E_{\text{meas}}(t)$  into this expression, followed by some simple arithmetic, yields

$$E'_{\text{meas}}(t) = E(t). \quad (6)$$

Thus it is trivial to obtain  $E(t)$  from the measured field. The pulse shown in Fig. 9 is the pulse from Fig. 8 with this simple procedure applied and shows remarkably good removal of the secondary pulse. As mentioned above, a more convenient algorithm could be developed as part of the FROG retrieval, and by including the multiple-pulse nature of the FROG trace inside the algorithm,  $E(t)$  could be retrieved directly from the trace.

Interestingly, it is possible to set up a version of this technique in which one can simply convert from standard FROG to POLKADOT FROG. It involves using an etalon at Brewster's angle with no coating on the second surface. As a result, the back surface will have a reflectivity of about 10% for the  $s$ -polarization and 0% for the  $p$ -polarization. The etalon should also be designed to have a 50% reflectivity for the  $s$ -polarization, and any reflectivity between about 25% and 75% for the  $p$ -polarization. As a result, an input pulse with  $s$ -polarization will be transformed to a train of pulses and will experience the POLKADOT effect, while a pulse with  $p$ -polarization will not and will experience a standard FROG measurement. Since it is very easy to rotate the polarization of a pulse before the FROG device (using a half-wave plate), this POLKADOT FROG arrangement could be very convenient.

Finally, a minor practical issue: of course, the relatively thick (off-the-shelf) optical elements of the etalon used in

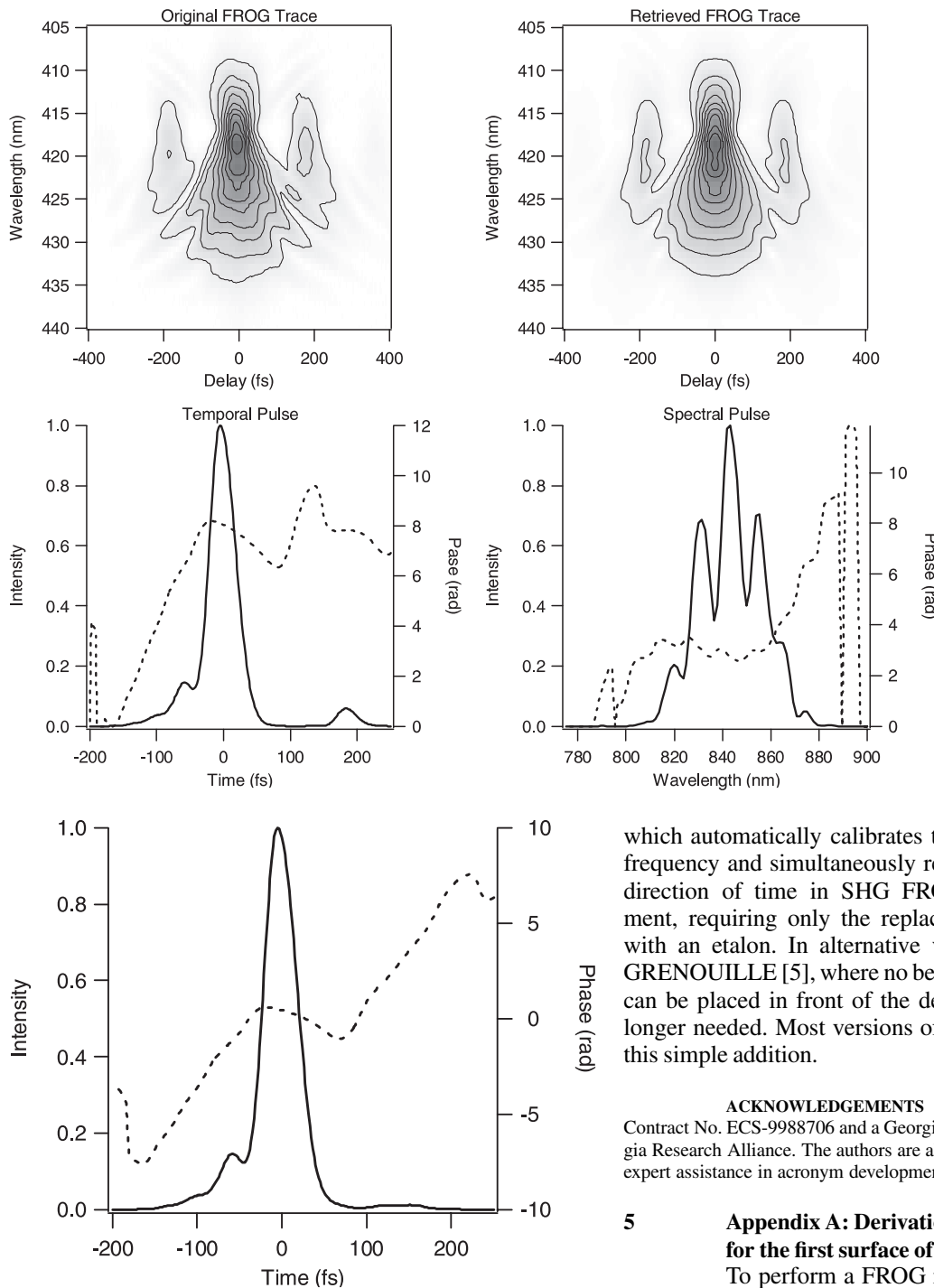


**FIGURE 9** The Retrieved Pulse Correction. The pulse after subtracting off the trailing pulses as described in (5). The secondary pulse is completely gone

this work distorted our pulse and would seriously distort extremely short pulses. Obviously, the thinner the elements used the less distortion will be present. For extremely short pulses, one could use an ultra-thin piece of glass as the etalon.

#### 4 Conclusions

To conclude, we have developed a simple variation of the FROG technique, called POLKADOT FROG,

**FIGURE 8** Retrieved POLKADOT FROG trace (top right) and retrieved pulse (bottom). This retrieval clearly shows the secondary pulse, indicating the direction of time

which automatically calibrates the device in both delay and frequency and simultaneously removes the ambiguity in the direction of time in SHG FROG. It is simple to implement, requiring only the replacement of the beam splitter with an etalon. In alternative versions of FROG, such as GRENOUILLE [5], where no beam splitter is used, the etalon can be placed in front of the device and removed when no longer needed. Most versions of FROG should benefit from this simple addition.

**ACKNOWLEDGEMENTS** This work was supported by NSF Contract No. ECS-9988706 and a Georgia Tech start-up grant from the Georgia Research Alliance. The authors are also grateful to Linda Trebino for her expert assistance in acronym development.

#### 5 Appendix A: Derivation of the 50% requirement for the first surface of the etalon

To perform a FROG measurement the two pulses must have identical shapes, but they can differ by a multiplicative factor without adversely affecting the measurement. In this paper, we have used the fact that only the first surface of the etalon needs to have a 50% reflectivity. It is not obvious that only the first surface is restricted and that the second surface is unrestricted. Given the schematic in Fig. 10, the following equations can be written for the two pulse trains:

$$\begin{aligned}
 I_1 &= (R_1 + T_1 R_2 T_1 + T_1 R_2 R_1 R_2 T_1 \\
 &\quad + T_1 R_2 (R_1 R_2)^2 T_1 + \dots) I_0 \\
 I_2 &= (T_2 T_1 + T_2 R_1 R_2 T_1 + T_2 (R_1 R_2)^2 T_1 \\
 &\quad + T_2 (R_1 R_2)^3 T_1 + \dots) I_0,
 \end{aligned} \tag{7}$$

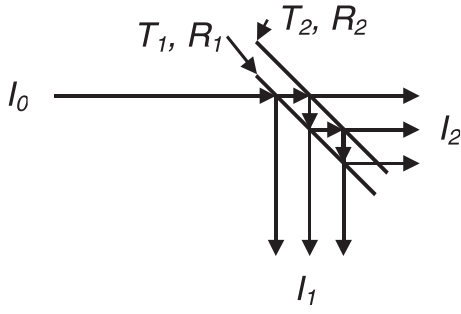


**FIGURE 10** Etalon Schematic. This is an exaggerated diagram of an etalon. The input beam,  $I_0$ , bounces between the two partially surfaces. Each round trip creates an attenuated, delayed replica of the input pulse

where  $T_i$  and  $R_i$  are the transmissions and reflectivities, respectively, of the first and second surfaces,  $I_0$  is the input intensity, and  $I_1$  and  $I_2$  are the transmitted intensities. We have not explicitly shown the delay factor in these equations; each element in the sum represents a pulse separated by  $\tau_{\text{sep}}$  from its neighbors. Factoring (7) yields

$$\begin{aligned} \frac{I_1}{I_0} &= R_1 \left( 1 + \frac{T_1^2 R_2}{R_1} \left( \sum_{i=0}^{\infty} (R_1 R_2)^i \right) \right) \\ \frac{I_2}{I_0} &= T_1 T_2 \left( 1 + R_1 R_2 \left( \sum_{i=0}^{\infty} (R_1 R_2)^i \right) \right) \end{aligned} \quad (8)$$

The  $R_1$  and  $T_1 T_2$  terms are unimportant for our purposes (they represent multiplicative factors). This means that, for both pulses to have the same shape, the following must hold true:

$$1 + \frac{T_1^2 R_2}{R_1} \left( \sum_{i=0}^{\infty} (R_1 R_2)^i \right) = 1 + R_1 R_2 \left( \sum_{i=0}^{\infty} (R_1 R_2)^i \right) . \quad (9)$$

From this equation, it is evident that the important factors are before the sum:

$$\frac{T_1^2 R_2}{R_1} = R_1 R_2 . \quad (10)$$

This yields the following condition:

$$T_1 = R_1 . \quad (11)$$

The only parameters remaining pertain to the first surface. For a loss-less interface,  $T = 1 - R$ , simplifying (11) to

$$R_1 = 1 - R_1 \quad (12)$$

$$R_1 = \frac{1}{2} \quad (13)$$

Therefore, if the first surface has a reflectivity of 50%, both pulse trains are identical.

**NOTE ADDED IN PROOF** During the course of this work we discovered a new ambiguity in SHG FROG. The following two pulses have the same SHG FROG trace: train of well separated pulses that potentially differ in peak intensity (e.g. a pulse train created by an etalon) and the same pulse train, but in which each individual pulse is reversed in time. This ambiguity is potentially inconvenient for the POLKADOT technique, but, fortunately, it is easy to remove. As long as there is some overlap between pulses in the train, we find that the SHG FROG traces of the above two pulse trains differ, removing the ambiguity. For instance the pulse in Fig. 8 has sufficient overlap. Indeed, it is difficult to avoid some overlap between pulses, so this ambiguity is unlikely to cause problems in POLKADOT FROG.

## REFERENCES

- 1 R. Trebino, K.W. DeLong, D.N. Fittinghoff, J.N. Sweetser, M.A. Krumb\u00fcgel, D.J. Kane: *Rev. Sci. Instrum.* **68**, 3277 (1997)
- 2 D.J. Kane, R. Trebino: *Opt. Lett.* **18**, 823 (1993)
- 3 R. Trebino, D.J. Kane: *J. Opt. Soc. Am. A* **10**, 1101 (1993)
- 4 G. Taft: private communication
- 5 P. O'Shea, M. Kimmel, X. Gu, R. Trebino: *Opt. Lett.* **26**, 932 (2001)